

Absolute Rates of Recombination and Disproportionation of Dimethylaminy Radicals

Yannis G. Lazarou and Panos Papagiannakopoulos*

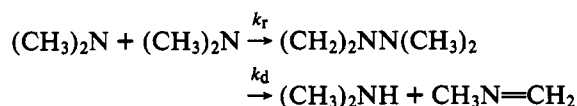
Department of Chemistry and Institute of Electronic Structure and Laser, University of Crete, and F.O.R.T.H., 71409 Heraklion, Crete, Greece

Received: April 14, 1993

The absolute rate constants for the recombination (k_r) and disproportionation (k_d) reactions of dimethylaminy radicals were determined at room temperature with the very low pressure reactor (VLPR) technique. The obtained values were $k_r = (1.70 \pm 0.19) \times 10^{-12} \text{ cm}^3 \text{ molecule}^{-1} \text{ s}^{-1}$ and $k_d = (4.19 \pm 0.52) \times 10^{-12} \text{ cm}^3 \text{ molecule}^{-1} \text{ s}^{-1}$, and the ratio k_d/k_r was 2.32 ± 0.26 . The transition-state geometries for both recombination and disproportionation reactions are loose, with the N...N bond length ca. 3.5 Å and the N...H...C distance ca. 4.4 Å. In the recombination TS, the four C–N...N bending modes are ca. 90 cm^{-1} and play a significant role in the formation of the N–N bond in tetramethylhydrazine. In the disproportionation TS, the two (in-plane and out-of-plane) vibrational modes of the metathetic hydrogen are ca. 110 cm^{-1} and are essential in the formation of the N–H bond in dimethylamine.

Introduction

The chemical reactivity of polyatomic organic free radicals in the gas phase is very important in combustion processes and in the photochemistry of polluted urban atmospheres. However, the rate constants of the fast recombination and disproportionation reactions of those radicals are often necessary, in order to determine their reactivity with other molecular species. In particular, the chemical reactivity of dialkylaminy radicals is very important to the homogeneous formation of carcinogenic nitrosamines in polluted atmospheres^{1,2,3} and the decomposition of nitramines.^{4,5} In general, radical–radical reactions are fast exothermic reactions with zero activation energy, resulting in recombination and disproportionation of the radicals.^{6,7} The self-reaction of dimethylaminy radicals has been studied in the past in both the gas⁸ and liquid⁹ phase and proceeds via recombination and disproportionation reactions



yielding tetramethylhydrazine (TMH) and dimethylamine (DMA). The yield of amine was always higher than that of hydrazine, and the ratio of rate constants k_r/k_d was less than 1. In the liquid phase the recombination reaction was totally suppressed under certain conditions.^{9c} The absolute rate constants of both reactions have been extrapolated from a photochemical reaction mechanism, and the reported values are $k_r = 2.83 \times 10^{-11} \text{ cm}^3 \text{ molecule}^{-1} \text{ s}^{-1}$ and $k_d = 1.90 \times 10^{-11} \text{ cm}^3 \text{ molecule}^{-1} \text{ s}^{-1}$.^{10,11} The total reaction rate has also been reported at the diffusion-controlled limit as $(3.3 \pm 1.7) \times 10^{-12} \text{ cm}^3 \text{ molecule}^{-1} \text{ s}^{-1}$.^{9b} However, the absolute rate constants k_r and k_d have not been measured in the past. Furthermore, the relative rate constants of the reaction of the dimethylaminy radical with NO, NO₂, and O₂ have been determined, and the reaction with NO is much faster than the reactions with O₂ and NO₂.¹²

In this work we will determine the absolute rate constants for the recombination and disproportionation reactions of dimethylaminy radicals, by using the very low pressure reactor (VLPR) technique.¹³

Experimental Section

Our experiments were performed with a very low pressure reactor (VLPR) apparatus, which has been described in great detail previously.¹⁴ The main characteristics of the system are

as follows: The bimolecular reaction is taking place in a Knudsen cell at steady-state pressures less than 5 mTorr. The reactants are flowing through separate capillaries (reaching uniform flows) and then are introduced into the reactor through separate inlets, where they are allowed to react for a short period of time. Both reactants and products are continuously discharged through a small aperture in the reactor to the first stage of a differentially pumped system. Therefore, a molecular flow is maintained leading to a collimated molecular beam that is sampled with a quadrupole mass spectrometer that is mounted in the second-stage vacuum chamber. The molecular beam is modulated with a tuning fork chopper at the entrance of the second vacuum chamber, so that the weak mass spectrometric signal can be magnified almost 1000 times with a lock-in amplifier.

Two different reaction cells were used in order to test the reproducibility of our results. The reaction cell was mounted on a stainless-steel flange containing a 5-mm aperture. The interior surfaces of the cell ($V = 225$ and 300 cm^3) were coated with halocarbon wax in order to inhibit wall recombination. The escape constant of the cells was measured by following the first-order decay curve (monitored by the mass spectrometer) for various gases after a fast halt of the flow. k_{escM} was found to be $1.67(T/M)^{1/2} \text{ s}^{-1}$ and $0.796(T/M)^{1/2} \text{ s}^{-1}$ respectively, where T is the absolute temperature and M is the molecular weight of the escaping species.

Dimethylaminy radicals (R) were produced by thermal decomposition of tetramethyl-2-tetrazene (TMT) diluted in He (5–10% mixture). The TMT/He mixture was introduced to the reaction cell through a cylindrical prechamber with 5-mm diameter and 1.5-cm length, where the decomposition was achieved by external thermal heating. The temperature was varied from 463 to 503 K, and the degree of TMT decomposition was limited in the range 72–1%. The total pressure in the prechamber is estimated to be less than 4 mTorr, and the dimethylaminy radical concentration was $(1-10) \times 10^{12} \text{ molecule/cm}^3$. However, the radical residence time in the heated prechamber is less than 1 ms, therefore all reaction is taking place in the Knudsen cell. This was further verified experimentally by blocking the exit orifice of the prechamber to the Knudsen cell (with an orifice of 1–2 mm) and by flowing NO₂ into the cell through another entrance (with smaller flow rates than He/TMT flows). This resulted in high yields of (CH₃)₂NNO₂, which is a primary reaction product.

Tetramethyl-2-tetrazene (TMT), tetramethylhydrazine (TMH), and dimethylamine (DMA) molecules were monitored by their

TABLE I. Typical Flow Rates of Helium Carrier Gas, Signal Intensities and Steady-State Concentrations of Tetramethyl-2-tetrazene, Tetramethylhydrazine, and Dimethylamine for Two Different Reaction Cells^a

F_{He} ($\times 10^{16}$)	ΔI_{TMT}	$\Delta[\text{TMT}]$ ($\times 10^{12}$)	$\Delta[\text{TMT}]/$ $[\text{TMT}]_0$	I_{TMT}	$[\text{TMT}]$ ($\times 10^{12}$)	I_{TMH}	$[\text{TMH}]$ ($\times 10^{11}$)	I_{DMA}	$[\text{DMA}]$ ($\times 10^{11}$)
$V_{\text{cell}} = 225 \text{ cm}^3$ and $k_{\text{escM}} = 1.67(T/M)^{1/2}$									
7.93	3.91	4.67	0.72	1.53	1.82	1.66	8.99	2.76	15.71
7.18	3.51	4.19	0.71	1.42	1.69	1.48	8.00	2.53	14.40
6.69	2.57	2.85	0.52	2.37	2.62	0.96	5.20	1.55	8.85
6.10	2.36	2.61	0.52	2.14	2.38	0.85	4.60	1.47	8.36
6.93	1.51	1.68	0.30	3.60	3.99	0.51	2.76	0.88	5.03
5.30	1.09	1.20	0.28	2.83	3.14	0.39	2.10	0.71	4.05
8.09	1.01	1.29	0.30	2.49	3.18	0.39	2.12	0.58	3.29
9.10	0.68	0.89	0.18	3.18	4.15	0.24	1.32	0.36	2.06
9.38	0.51	0.67	0.13	3.46	4.52	0.17	0.90	0.25	1.39
9.48	0.07	0.09	0.02	3.89	5.15	0.01	0.05	0.01	0.07
$V_{\text{cell}} = 300 \text{ cm}^3$ and $k_{\text{escM}} = 0.796(T/M)^{1/2}$									
6.78	1.21	3.57	0.41	1.73	5.13	0.62	7.34	1.56	14.07
6.93	1.26	3.73	0.42	1.74	5.15	0.67	7.94	1.48	13.35
6.96	1.00	2.97	0.33	2.01	5.94	0.51	6.10	1.19	10.70
7.51	0.77	2.27	0.24	2.48	7.35	0.33	3.96	0.91	8.23
3.94	0.87	2.15	0.43	1.16	2.87	0.37	4.39	0.82	7.32
3.91	0.84	2.07	0.42	1.18	2.92	0.37	4.41	0.78	6.95
3.84	0.57	1.42	0.29	1.41	3.47	0.24	2.89	0.51	4.53
3.77	0.31	0.76	0.16	1.64	4.05	0.10	1.23	0.24	2.10
3.67	0.20	0.49	0.10	1.70	4.20	0.05	0.59	0.12	1.10
3.57	0.05	0.13	0.03	1.79	4.42	0.01	0.12	0.02	0.16

^a Helium carrier gas flow is in molecule s^{-1} , steady-state concentrations are in molecule cm^{-3} . Signal intensities are in arbitrary units normalized relative to the mass spectrometer and lock-in amplifier sensitivities used.

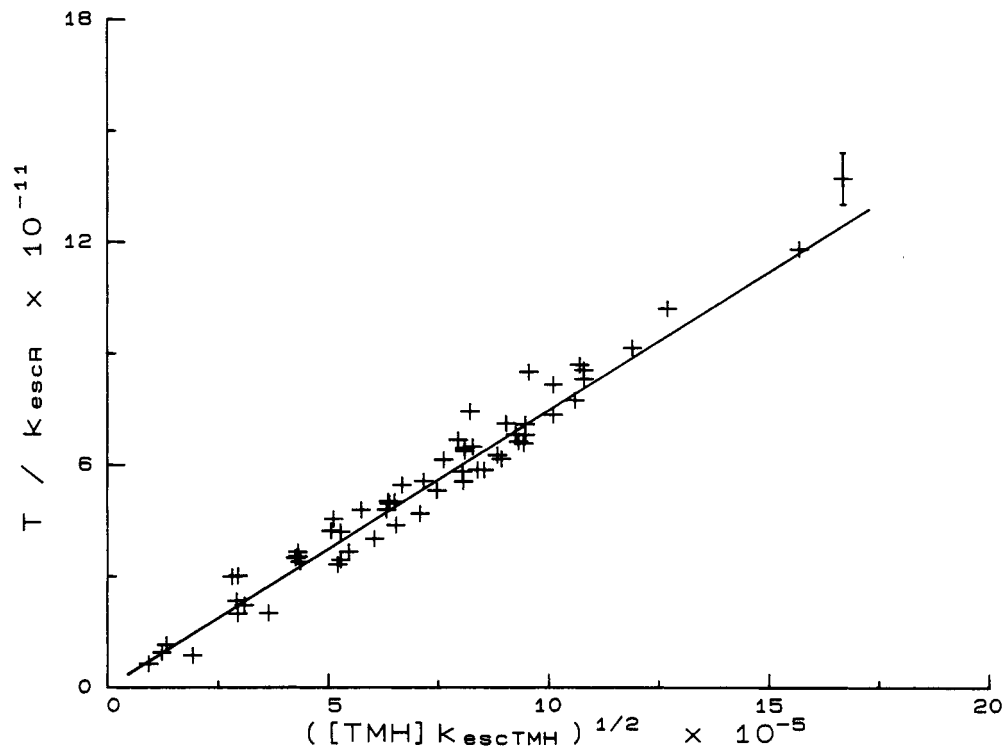


Figure 1. Plot of T/k_{escR} versus $([\text{TMH}]k_{\text{escTMH}})^{1/2}$ at 303 K, where $T = 2\{\Delta[\text{TMT}]k_{\text{escTMT}} - ([\text{TMH}]k_{\text{escTMH}} + [\text{DMA}]k_{\text{escDMA}})\}$. Symbol size reflects the propagated errors (2σ).

TABLE II: Recombination, Disproportionation, and Total Rate Constant Values for Dimethylaminyl Radical Reactions. (Units in $\text{cm}^3 \text{ molecule}^{-1} \text{ s}^{-1}$)

$k_r (\times 10^{12})$	$k_d (\times 10^{12})$	$k_r + k_d (\times 10^{12})$	reference
1.70 ± 0.19	4.19 ± 0.52	5.89 ± 0.55	this work
28.3	19	47.3	11
27.8	4.5	32.3	10
		3.3 ± 1.7	9b

parent mass spectrum peaks, I_{TMT} (m/e 116), I_{TMH} (m/e 88), and I_{DMA} (m/e 45), respectively. The observed peak intensities $I_M = \alpha_M F_M = \alpha_M V k_{\text{escM}} [\text{M}]$, where α_M is a calibration factor characteristic of each molecule, F_M is the flow rate, V is the cell

volume, k_{escM} is the escape rate, and $[\text{M}]$ is the steady-state concentration in the reaction cell. Hence, the steady-state concentration $[\text{M}]$ can be determined by knowing V , k_{escM} , and the α_M factor. It is therefore necessary to obtain accurate calibration curves, I_M versus F_M , in order to determine the α_M factors for TMT, TMH, and DMA. The flow rates F_{TMT} , F_{TMH} , and F_{DMA} were determined by monitoring the pressure drop in a known volume, with an accuracy of ca. $\pm 5\%$. In each experimental run the intensities of all mass spectrum peaks of interest were recorded simultaneously and stored digitally in a microcomputer (PDP-11/23), where the analysis was consequently performed. Finally, the system was tested by measuring the rate constant of the well-known reaction of Cl with CH_4 , and

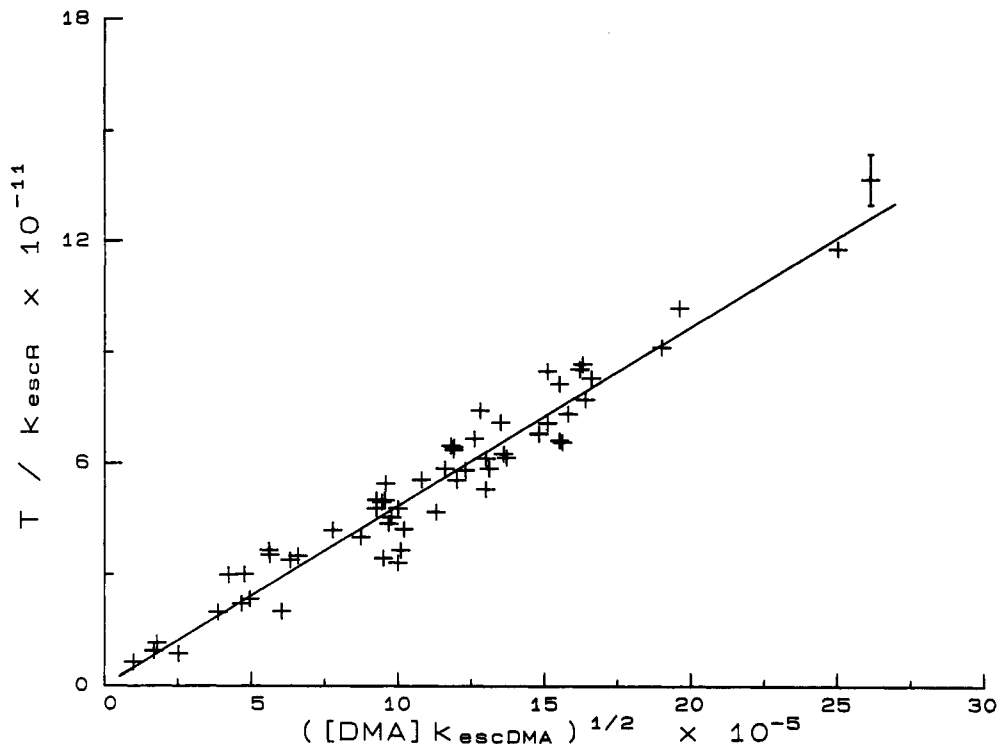


Figure 2. Plot of T/k_{escR} versus $([\text{DMA}]k_{\text{escDMA}})^{1/2}$ at 303 K, where $T = 2 \{ \Delta[\text{TMT}]k_{\text{escTMT}} - ([\text{TMH}]k_{\text{escTMH}} + [\text{DMA}]k_{\text{escDMA}}) \}$. Symbol size reflects the propagated errors (2σ).

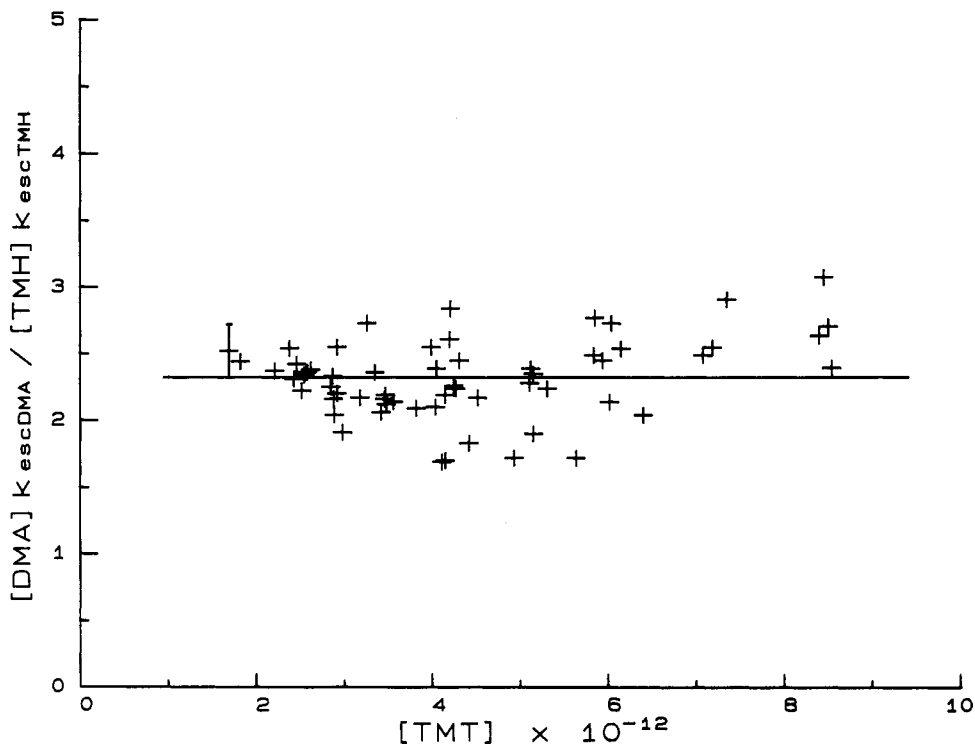


Figure 3. Plot of $([\text{DMA}]k_{\text{escDMA}})/([\text{TMH}]k_{\text{escTMH}})$ versus $[\text{TMT}]$ at 303 K. Symbol size reflects the propagated errors (2σ).

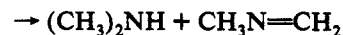
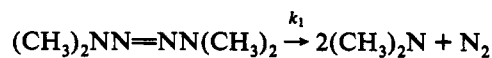
the obtained rate at 303 K was in excellent agreement with the accepted value.¹⁵

Tetramethyl-2-tetrazene, $(\text{CH}_3)_2\text{NN}=\text{NN}(\text{CH}_3)_2$, was prepared by the procedure of Madginski et al.¹⁶ Tetramethylhydrazine and dimethylamine were commercially available (Fluka and Aldrich) and were degassed several times prior to use.

Results

The mass spectroscopic analysis of the reaction products shows the formation of dimethylamine ($m/e = 45$) and tetramethyl-

hydrazine ($m/e = 88$). Thus, the reaction scheme is as follows



The steady-state approximations for the tetramethyl-2-tetrazene, dimethylaminy radical, dimethylamine, and tetramethyl-

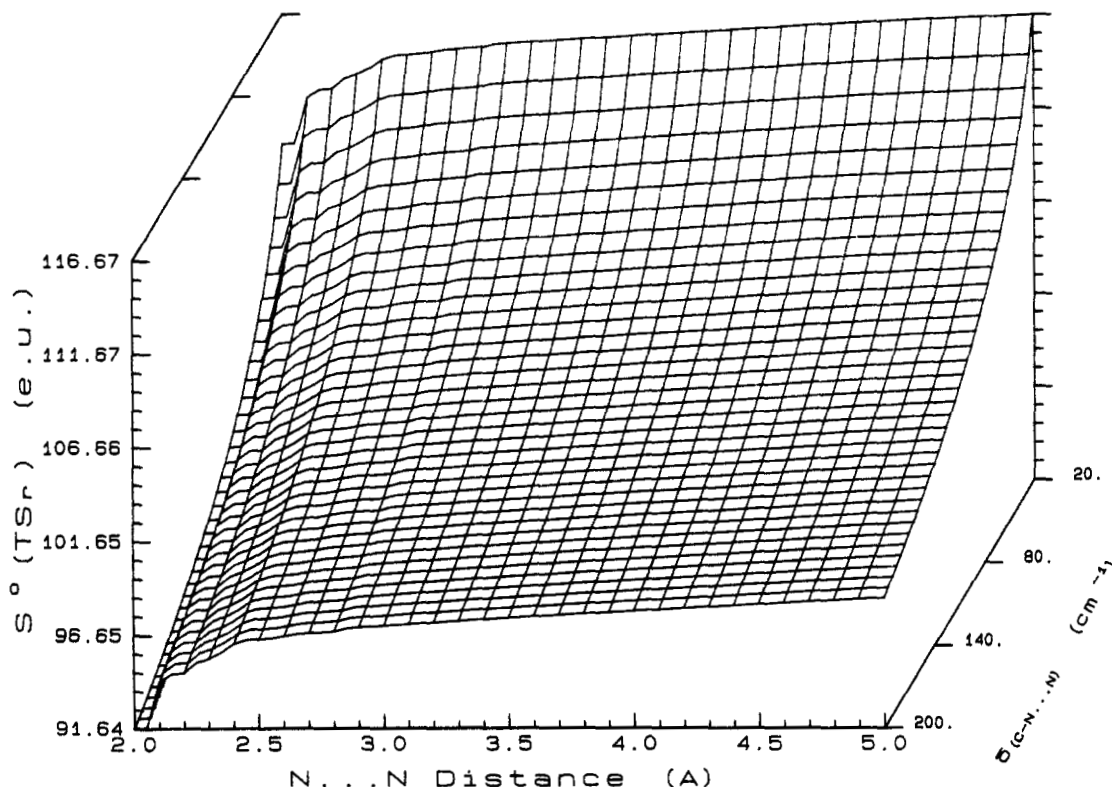


Figure 4. Absolute entropy of the transition-state complex, $S^\circ(TS_r)$, for the recombination of dimethylaminy radicals, as a function of the N...N distance and the $\delta(C-N\cdots N)$ bending frequency.

ylhydrazine species are given respectively by the expressions:

$$k_1[\text{TMT}] = \Delta[\text{TMT}]k_{\text{escTMT}} \quad (\text{I})$$

$$2\Delta[\text{TMT}]k_{\text{escTMT}} = 2(k_r + k_d)[\text{R}]^2 + k_{\text{escR}}[\text{R}] \quad (\text{II})$$

$$k_r[\text{R}]^2 = k_{\text{escTMH}}[\text{TMH}] \quad (\text{III})$$

$$k_d[\text{R}]^2 = k_{\text{escDMA}}[\text{DMA}] \quad (\text{IV})$$

where $\Delta[\text{TMT}]$ is the change in the TMT steady-state concentration (in molecule/cm³) in the reactor; $[\text{TMH}]$ and $[\text{DMA}]$ are the steady-state concentrations (in molecule/cm³) of TMH and DMA, respectively. k_{escM} are the escape constants of all species out of the reactor. Furthermore, combination of the above expressions yields:

$$2\{\Delta[\text{TMT}]k_{\text{escTMT}} - ([\text{TMH}]k_{\text{escTMH}} + [\text{DMA}]k_{\text{escDMA}})\} = k_{\text{escR}}[\text{R}]$$

where $[\text{R}]$ can be substituted either by expression III or IV and give

$$T = 2\{\Delta[\text{TMT}]k_{\text{escTMT}} - ([\text{TMH}]k_{\text{escTMH}} + [\text{DMA}]k_{\text{escDMA}})\} \\ = k_{\text{escR}}([\text{TMH}]k_{\text{escTMH}})^{1/2}/(k_r)^{1/2} \quad (\text{V})$$

$$T = 2\{\Delta[\text{TMT}]k_{\text{escTMT}} - ([\text{TMH}]k_{\text{escTMH}} + [\text{DMA}]k_{\text{escDMA}})\} \\ = k_{\text{escR}}([\text{DMA}]k_{\text{escDMA}})^{1/2}/(k_d)^{1/2} \quad (\text{VI})$$

Therefore, the plots of T/k_{escR} versus $([\text{TMH}]k_{\text{escTMH}})^{1/2}$ and

$([\text{DMA}]k_{\text{escDMA}})^{1/2}$ should yield straight lines with slopes equal to $k_r^{-1/2}$ and $k_d^{-1/2}$, respectively, with zero intercept.

Experiments were performed at different degrees of TMT decomposition ($\Delta[\text{TMT}]$) by varying the decomposition temperature. Typical flow rates of He carrier gas, peak intensities, and steady-state concentrations of TMT, TMH, and DMA at various degrees of TMT decomposition and two different reaction cells are presented in Table I. The above plots at 303 K yield straight lines with zero intercept, as can be seen in Figures 1 and 2. The linear least-squares fits of 60 points from 5 different experiments yield the slopes, which further provide the rate constant values at 303 K for both recombination and disproportionation reactions

$$k_r = (1.70 \pm 0.19) \times 10^{-12} \text{ cm}^3 \text{ molecule}^{-1} \text{ s}^{-1}$$

$$k_d = (4.19 \pm 0.52) \times 10^{-12} \text{ cm}^3 \text{ molecule}^{-1} \text{ s}^{-1}$$

with an accuracy 2σ .

Finally, the ratio of expressions IV and III gives

$$k_d/k_r = [\text{DMA}]k_{\text{escDMA}}/[\text{TMH}]k_{\text{escTMH}} \quad (\text{VII})$$

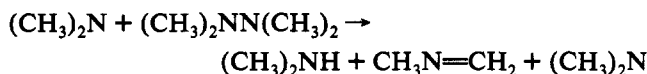
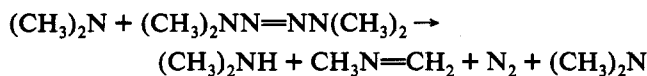
which should be independent of TMT concentration. Indeed, a plot of $[\text{DMA}]k_{\text{escDMA}}/[\text{TMH}]k_{\text{escTMH}}$ versus $[\text{TMT}]$ yields a straight line, as shown in Figure 3, and the ratio $k_d/k_r = 2.32 \pm 0.26$ with an accuracy 2σ . This is in agreement with the ratio 2.46 ± 0.41 of the rate constant values.

Discussion

In the reaction products the formation of amine was always greater than hydrazine, and this could be attributed to the presence of the secondary reactions

TABLE III: Estimation of the S^{\ddagger}_{298} of the Dimethylaminy Radical

degrees of freedom		S° , cal mol ⁻¹ K ⁻¹
translational $S_{tr} = 37.0 + (3R/2) \ln(M^{\ddagger}/40)$ ($M = 44$ amu)		37.28
rotational $S_{ext,rot} = 11.595 + (R/2) \ln(I_A I_B I_C) - R \ln \sigma$ ($I_A I_B I_C = 3.467 \times 10^4$ amu ³ Å ⁶ , $\sigma = 2$, symmetry group C_{2v})		20.62
vibrational		
assignment	frequencies (cm ⁻¹)	
(2) t _{C-N}	230 ($I_r = 2.9$ amu Å ² , $V = 2.9$ kcal/mol)	3.8
$\nu_{C-N} + \delta_{H-C-N}$	345	1.22
$\nu_{C-N} + \delta_{H-C-N} + t_{CH_3}$	450	0.81
$\nu_{C-N} + \delta_{H-C-N} + \delta_{H-C-H}$	860	0.17
ν_{C-N}	950	0.12
$\nu_{C-N} + \delta_{H-C-N}$	1000	0.1
δ_{H-C-N}	1080	0.07
$\delta_{C-N-C} + \delta_{H-C-N} + \nu_{C-N}$	1163	0.05
$\delta_{C-N-C} + \delta_{H-C-N}$	1172	0.05
$\nu_{C-N} + \delta_{H-C-N}$	1290	0.03
$\delta_{H-C-H} + \delta_{H-C-N}$	1418	0.02
$\delta_{H-C-H} + \delta_{H-C-N}$	1420	0.02
$\delta_{H-C-H} + \delta_{N-C-N} + \nu_{C-N}$	1483	0.01
$\delta_{H-C-N} + \delta_{C-N-C} + \nu_{C-N}$	1610	0.007
ν_{C-H}	2820	0.0
ν_{C-H}	2822	0.0
ν_{C-H}	2956	0.0
ν_{C-H}	2957	0.0
ν_{C-H}	2958	0.0
ν_{C-H}	2960	0.0
electronic $S_{el} = R \ln(2S+1)$ ($S = 1/2$)		1.39
		65.77



However, this possibility is excluded by the fact that the ratio $[\text{DMA}]k_{\text{escDMA}}/[\text{TMH}]k_{\text{escTMH}}$ is always constant for various TMT concentrations, as can be seen in Figure 3. The absence of the above reactions was also demonstrated by flowing pure TMT or TMH into the reaction cell through the second inlet, and this did not produce any increase in the dimethylamine yield. Thus, the observed amine and hydrazine molecules are primary reaction products.

The obtained k_r and k_d values can be compared with previous values obtained by flash photolysis of dimethylacetamide¹⁰ and dimethylhydrazine¹¹ in the gas phase and are presented in Table II. In general, our rate constant values are lower by an order of magnitude, except the disproportionation rate which is equal with a previous value.¹⁰ The total reaction rate is in good agreement with a previous value obtained by thermolysis or photolysis of tetramethyl-2-tetrazene in solution.^{9b} Finally, the obtained k_d/k_r value is higher than 1, which is in agreement with previous values of ≈ 1.2 in the gas phase^{8a} and 1.44 in the liquid phase^{9c} but in disagreement with an extrapolated value of 0.6 in the gas phase.¹¹

The thermochemical kinetics version of conventional transition-state theory¹⁷ can be applied to both recombination and disproportionation reactions, in order to provide some insight about the two transition-state geometries. In general, radical recombination and disproportionation reactions appear to have little or no activation energy,¹⁸ therefore the preexponential A factors are equal to the corresponding rate constant values. However, the A factors can be expressed as

$$A = 10^{-5.72}(T/298)^2 \exp(\Delta S^{\ddagger}/R)$$

where ΔS^{\ddagger} is the entropy change for forming one mole of transition-state complex from the reactants,¹⁸ and in this case is

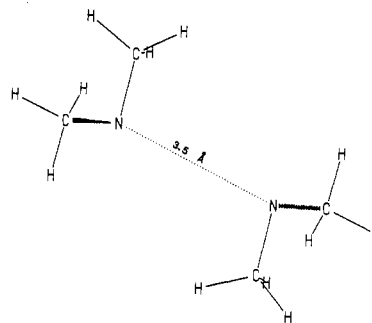


Figure 5. Transition-state geometry for the recombination of two dimethylaminy radicals.

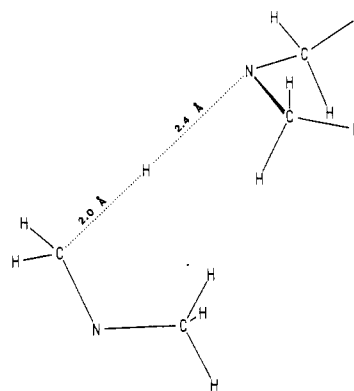


Figure 6. Transition-state geometry for the disproportionation of two dimethylaminy radicals.

$\Delta S^{\ddagger} = S^{\circ}\{\text{TS}\} - 2 S^{\circ}\{(\text{CH}_3)_2\text{N}\}$. Estimation of the absolute entropies for both reactants and transition states requires knowledge of their geometry and their vibrational frequencies. For the dimethylaminy radical the absolute entropy was estimated by adopting the reported geometry¹⁹ and by assigning the vibrational frequencies. The force constants of dimethylamine²⁰ were used in order to estimate the radical frequencies, and their assignment is presented in Table III. The obtained value is $S^{\circ}\{(\text{CH}_3)_2\text{N}\} = 65.8$ cal/(mol K), which is in good agreement with

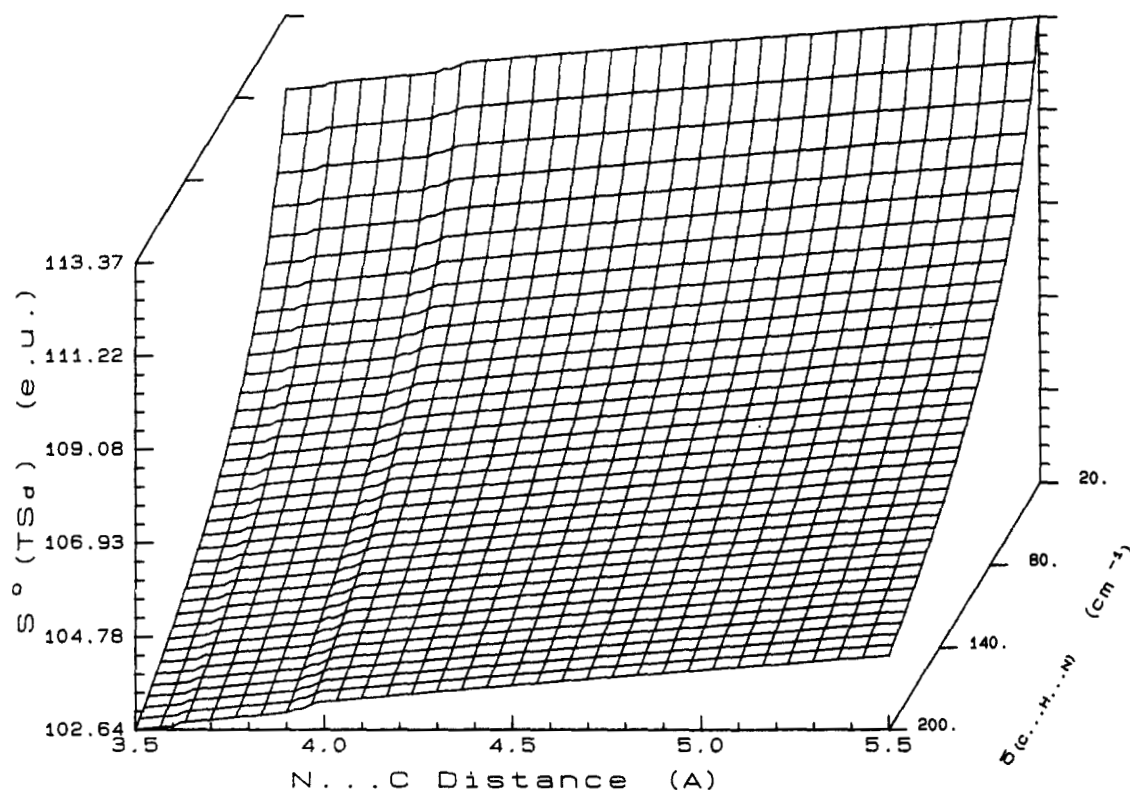


Figure 7. Absolute entropy of the transition-state complex, $S^\circ(\text{TS}_d)$, for the disproportionation of dimethylaminy radicals, as a function of the $\text{N}\cdots\text{H}\cdots\text{C}$ distance and the $\delta(\text{N}\cdots\text{H}\cdots\text{C})$ bending frequency.

TABLE IV: Estimation of the S°_{298} for the Recombination Transition State

degrees of freedom		S° , cal mol ⁻¹ K ⁻¹
translational $S_{tr} = 37.0 + (3R/2) \ln(M^*/40)$ ($M = 88$ amu)		39.36
rotational $S_{ext,rot} = 11.595 + (R/2) \ln(I_A I_B I_C) - R \ln \sigma$ ($I_A I_B I_C = 2.27 \times 10^7$ amu ³ Å ⁶ , $\sigma = 1$)		28.45
vibrational		
radical	transition state (cm ⁻¹)	
(2) $\nu_{\text{C-N}} + \delta_{\text{H-C-N}}$	345	2.44
(2) $\nu_{\text{C-N}} + \delta_{\text{H-C-N}} + \nu_{\text{CH}_3}$	450	1.62
(2) $\nu_{\text{C-N}} + \delta_{\text{H-C-N}} + \delta_{\text{H-C-H}}$	860	0.34
(2) $\nu_{\text{C-N}}$	950	0.24
(2) $\nu_{\text{C-N}} + \delta_{\text{H-C-N}}$	1000	0.2
(2) $\delta_{\text{H-C-N}}$	1079	0.14
(2) $\delta_{\text{C-N-C}} + \delta_{\text{H-C-N}} + \nu_{\text{C-N}}$	1163	0.1
(2) $\delta_{\text{C-N-C}} + \delta_{\text{H-C-N}}$	1172	0.1
(2) $\nu_{\text{C-N}} + \delta_{\text{H-C-N}}$	1290	0.06
(4) $\nu_{\text{C-N}}$ (230 cm ⁻¹)	220	7.96
($V = 2.9$ kcal/mol, $I_r = 2.9$ amu Å ²)	(4) $\nu_{\text{C-N}}$ ($V = 2.9$ kcal/mol, $I_r = 3.2$ amu Å ²)	
	$\nu_{\text{N-N}}$ (r.c.)	
	(4) $\delta_{\text{C-N-N}}$	14.78
	free internal rotation about $\text{N}\cdots\text{N}$ ($I_r = 31.64$ amu Å ² , $\text{N}\cdots\text{N} \approx 3.5$ Å)	8.03
electronic $S_{el} = R \ln(2S+1)$ ($S = 0$)		0
		103.8

$$\Delta S^\circ(298) = 103.8 - 2 \times 65.8 = -27.8 \text{ e.u.}$$

$$A_{300} (\text{cm}^3 \text{ molecule}^{-1} \text{ s}^{-1}) = 10^{-5.72} (T/298)^2 \exp(\Delta S^\circ/R) = 1.69 \times 10^{-12} = 10^{-11.77}$$

the previously estimated value of 65.3 cal/(mol K).²¹ The absolute entropies of both transition states can be obtained from the experimental rates and must be reproduced by assigning the geometry and the vibrational frequencies of both transition states.

For the recombination reaction the obtained rate constant value corresponds to an entropy change $\Delta S^\circ = -27.79$ cal/(mol K), which correlates to an absolute entropy $S^\circ(\text{TS}_r) = 103.8$ cal/(mol K). The recombination transition state is formed by coupling the unpaired electrons of nitrogen atoms from both radicals, thus the $\text{C-N}\cdots\text{N}$ angle will be ca. 110°. This TS is expected to be "loose" like in the inverse process of unimolecular decomposition

of tetramethylhydrazine, where the TS has an $\text{N}\cdots\text{N}$ bond length of 3.5 Å.²² The rotational entropy of the TS shows very little dependence (≈ 0.5 cal/(mol K)) on the $\text{N}\cdots\text{N}$ bond length from 3 to 5 Å, and so does $S^\circ(\text{TS}_r)$ as can be seen in Figure 4. For $\text{N}\cdots\text{N}$ distances shorter than 3 Å there is a decrease in $S^\circ(\text{TS}_r)$ and a steric hindrance in the rotation of TS around the $\text{N}\cdots\text{N}$ axis, which is due to an overlap of the van der Waals radii of hydrogen atoms of the approaching radicals. Thus, the TS geometry for the recombination of two dimethylaminy radicals is presented in Figure 5. The vibrational frequencies of the TS are similar and twice the number of those in the radical, plus six

TABLE V: Estimation of the S^\ddagger_{298} for the Disproportionation Transition State

degrees of freedom		S° , cal mol ⁻¹ K ⁻¹
translational $S_{tr} = 37.0 + (3R/2) \ln(M^*/40)$ ($M = 88$ amu)		39.36
rotational $S_{ext,rot} = 11.595 + (R/2) \ln(I_A I_B I_C) - R \ln \sigma$ ($I_A I_B I_C = 3.116 \times 10^7$ amu ³ Å ⁶ , $\sigma = 1$)		28.76
vibrational		
radical	transition state (cm ⁻¹)	
ν_{C-H} (2900 cm ⁻¹) →	ν_{C-H} (r.c.)	
(2) δ_{H-C-H} (1420 cm ⁻¹) →	(2) δ_{H-C-H} 286	3.06
δ_{H-C-N} (1080 cm ⁻¹) →	δ_{H-C-N} 230	1.90
(2) $\nu_{C-N} + \delta_{H-C-H}$ →	345	2.44
(2) $\nu_{C-N} + \delta_{H-C-N} + t_{CH_3}$ →	450	1.62
(2) $\nu_{C-N} + \delta_{H-C-H} + \delta_{H-C-N}$ →	860	0.34
(2) ν_{C-N} →	950	0.24
(2) $\nu_{C-N} + \delta_{H-C-N}$ →	1000	0.2
δ_{H-C-N} →	1079	0.07
(2) $\delta_{C-N-C} + \delta_{H-C-N} + \nu_{C-N}$ →	1163	0.1
(2) $\delta_{C-N-C} + \delta_{H-C-N}$ →	1172	0.1
(2) $\nu_{C-N} + \delta_{H-C-N}$ →	1290	0.06
(3) t_{C-N} (230 cm ⁻¹) →	(3) t_{C-N} 220	5.97
($V = 2.9$ kcal/mol, $I_r = 2.9$ amu Å ²)	($V = 2.9$ kcal/mol, $I_r = 3.2$ amu Å ²)	
t_{C-N} (230 cm ⁻¹) →	t_{C-N} 186	2.3
($V = 2.9$ kcal/mol, $I_r = 2.9$ amu Å ²)	($V = 15$ kcal/mol, $I_r = 30.5$ amu Å ²)	
	ν_{N-H} 670	0.35
	(2) δ_{C-N-H} 220	3.98
	(2) δ_{N-H-C} 110	6.61
	free internal rotation about N...C ($I_r = 40.73$ amu Å ² , $N...C \approx 4.4$ Å)	8.28
electronic $S_{el} = R \ln(2S+1)$ ($S = 0$)		0
		105.7

$$\Delta S^\ddagger(298) = 105.7 - 2 \times 65.8 = -25.9 \text{ e.u.}$$

$$A_{300} (\text{cm}^3 \text{ molecule}^{-1} \text{ s}^{-1}) = 10^{-5.72} (T/298)^2 \exp(\Delta S^\ddagger/R) = 4.39 \times 10^{-12} = 10^{-11.36}$$

new vibrations. However, the vibrational entropy depends strongly on the four new $\delta(C-N...N)$ bending modes of low frequency, which are adjusted in order to reproduce the experimental data, see Figure 4. The resulting value for those low-frequency modes is ca. 90 cm⁻¹. The internal rotation around the N...N bond is treated as a free rotor (one dimension). All vibrational frequency assignments for the TS and the entropy calculations are included in Table IV.

In a similar manner the disproportionation rate constant corresponds to an entropy change $\Delta S^\ddagger = -25.99$ cal/(mol K), which further correlates to an absolute entropy $S^\circ(TS_\ddagger) = 105.6$ cal/(mol K). The disproportionation transition-state geometry is formed by coupling one nitrogen unpaired electron with a hydrogen of another radical, thus the C-N...H angle will be ca. 105°. The relative orientation of the approaching radicals is guided by their dipole-dipole interaction, and the approach with the minimum repulsion is achieved when the planes of the two radicals (defined by nitrogen and two carbons) are perpendicular. The critical distance of approach takes place when the van der Waals spheres of the two radicals come in contact, and this occurs when the distance between the N* radical and an H atom from a neighboring radical becomes ca. 2 Å.²³ For N...H...C distances shorter than 3 Å there is a decrease in $S^\circ(TS_\ddagger)$ and a steric hindrance in the rotation of TS around the N...C axis. The TS geometry for the disproportionation of two dimethylaminy radicals is presented in Figure 6. The vibrational frequencies of the TS are similar and twice the number of those in the radical, except for the bending frequencies (two H...C-H and one H...C-N) which are reduced by 80% and the stiffening of the torsion around the C-N bond. In addition, there are six new vibrational frequencies: one N...H stretching and two C-N...H bending modes which are also reduced by 80% relative to their value in dimethylamine,²⁰ one internal free rotation around the N...C axis, and the in-plane and out-of-plane motions of the H atom, $\delta(N...H...C)$. The frequency of the latter modes is adjusted in

order to reproduce the experimental value of $S^\circ(TS_\ddagger)$. Therefore, a plot of $S^\circ(TS_\ddagger)$ as a function of the N...C distance and the $\delta(N...H...C)$ frequency is drawn and presented in Figure 7. The resulting value for those low-frequency modes is ca. 110 cm⁻¹. All vibrational frequency assignments and entropy calculations are included in Table V.

The recombination and disproportionation reactions of dimethylaminy radicals are exothermic by ca. 60 kcal/mol and 64 kcal/mol, respectively, assuming that $\Delta H^\circ_f((CH_3)_2N) = 38.2$ kcal/mol,²⁴ $\Delta H^\circ_f((CH_3)_2NN(CH_3)_2) = 16$ kcal/mol,²⁵ $\Delta H^\circ_f(CH_3N=CH_2) = 17.3$ kcal/mol,²⁶ and $\Delta H^\circ_f((CH_3)_2NH) = -4.7$ kcal/mol.¹⁷ The recombination reaction probably has a zero activation energy, thus the A_r factor will be given by the expression¹⁷

$$\ln A_r = \ln A_{dec} - \Delta S^\circ/R$$

where ΔS° is the entropy change for the reverse reaction of TMH decomposition. $\Delta S^\circ = 47.6$ cal/(mol K), since $S^\circ_{300}((CH_3)_2NN(CH_3)_2) = 84$ cal/(mol K) and $S^\circ_{300}((CH_3)_2N) = 65.8$ cal/(mol K). The high-pressure A factor for TMH decomposition (A°_{dec}) has been determined from pyrolysis experiments as $10^{17.4}$ s⁻¹,²² thus $A^\circ_{r(300)} \approx 1.4 \times 10^{-12}$ cm³ molecule⁻¹ s⁻¹. This high-pressure limit value of A_r is in excellent agreement with the experimentally obtained value.

Conclusions

The absolute rate constant values for the recombination and disproportionation of two dimethylaminy radicals have been determined at 303 K. The disproportionation reaction is 2.32 times faster than the recombination reaction. The conventional transition-state theory reveals that both reactions proceed through very loose transition states, where the N...N distance in recombination is ca. 3.5 Å and the N...H...C distance in disproportionation is ca. 4.4 Å. Finally, both transition states contain

several new bending modes of low frequency, which are estimated to be ca. 100 cm⁻¹, and play a significant role in both reaction processes.

Acknowledgment. This work was performed in the frame of a NATO Collaborative Research Grant (CGR 900054) with Professor Sidney W. Benson whose contribution is greatly acknowledged. It was also supported by the University of Crete Research Committee.

Registry No. The following registry numbers were supplied by the author. Dimethylaminy radical, 15337-44-7; tetramethyl-2-tetrazene, 6130-87-6; tetramethylhydrazine, 6415-12-9; dimethylamine, 124-40-3; *N*-methylmethyleimine, 1761-67-7.

References and Notes

- (1) Graedel, T. E.; Hawkins, D. T.; Claxton, L. D. *Atmospheric Chemical Compounds*; Academic Press, Inc.: London, 1986.
- (2) U. S. Environmental Protection Agency, Scientific and Technical Assessment Report on Nitrosamines. Report No. EPA-600/6-77-001; November, 1976.
- (3) Hanst, P. L.; Spence, J. W.; Miller, M. *Environ. Sci. Technol.* **1977**, *11*, 403.
- (4) Lazarou, Y. G.; Papagiannakopoulos, P. *J. Phys. Chem.* **1990**, *94*, 7114.
- (5) Lazarou, Y. G.; King, K. D.; Papagiannakopoulos, P. *J. Phys. Chem.* **1992**, *96*, 7351.
- (6) Benson, S. W. *Acc. Chem. Res.* **1986**, *19*, 335.
- (7) Benson, S. W. *Can. J. Chem.* **1983**, *61*, 881.
- (8) (a) Watson, J. S. *J. Chem. Soc.* **1956**, 3677. (b) Gesser, H.; Mullhaupt, J. T.; Griffiths, J. E. *J. Am. Chem. Soc.* **1957**, *79*, 4834. (c) Jones, P. W.; Gesser, H. D. *J. Chem. Soc. B* **1971**, 1877.
- (9) (a) Roberts, J. R.; Ingold, K. U. *J. Am. Chem. Soc.* **1971**, *93*, 6686; (b) **1973**, *95*, 3228. (c) Hancock, K. G.; Dickinson, D. A. *J. Org. Chem.* **1975**, *40*, 969.
- (10) Seetula, J.; Blomqvist, K.; Kalliorinne, K.; Koskikallio, J. *Acta Chem. Scand. A* **1986**, *40*, 658.
- (11) Seetula, J.; Kalliorinne, K.; Koskikallio, J. *J. Photochem. Photobiol. A* **1988**, *43*, 31.
- (12) Lindley, C. R. C.; Calvert, J. G.; Shaw, J. H. *Chem. Phys. Lett.* **1979**, *67*, 57.
- (13) Golden, D. M.; Spokes, G. N.; Benson, S. W. *Angew. Chem., Int. Ed. Engl.* **1973**, *12*, 534.
- (14) (a) Lazarou, Y. G.; Michael, C.; Papagiannakopoulos, P. *J. Phys. Chem.* **1992**, *96*, 1705. (b) Lazarou, Y. G.; Papagiannakopoulos, P. *J. Phys. Chem.* **1993**, *97*, 4468.
- (15) DeMore, W. B.; Molina, M. J.; Watson, R. T.; Golden, D. M.; Hampson, R. F.; Kurylo, M. J.; Howard, C. J.; Ravishankara, A. R. *Chemical Kinetics and Photochemical Data for Use in Stratospheric Modelling*. J.P.L. Publication 90-1; Jet Propulsion Laboratory, California Institute of Technology: Pasadena, CA, 1990.
- (16) Madginski, L. J.; Pilay, K. S.; Richard, H.; Chow, Y. L. *Can. J. Chem.* **1978**, *56*, 1657.
- (17) Benson, S. W. *Thermochemical Kinetics*, 2nd ed.; Wiley-Interscience: New York, 1976.
- (18) (a) Benson, S. W. *Acc. Chem. Res.* **1986**, *19*, 335. (b) Benson, S. W. *Can. J. Chem.* **1983**, *61*, 881.
- (19) Owen, F. J.; Vogel, V. L. *J. Chem. Phys.* **1976**, *64*, 851.
- (20) Dellepiane, G.; Zerbi, G. *J. Chem. Phys.* **1968**, *48*, 3573.
- (21) Stein, S. E.; Rukkers, J. M.; Brown, R. L. *NIST Structures and Properties Database and Estimation Program, NIST Standard Reference Database 25, National Standards and Technology*; Gaithersburg, MD, 20899, 1991.
- (22) Golden, D. M.; Solly, R. K.; Gac, N. A.; Benson, S. W. *Int. J. Chem. Kinet.* **1972**, *4*, 433.
- (23) Benson, S. W. *J. Phys. Chem.* **1985**, *89*, 4366.
- (24) Golden, D. M.; Solly, R. K.; Gac, N. A.; Benson, S. W. *J. Am. Chem. Soc.* **1972**, *94*, 363.
- (25) Gowenlock, B. G.; Jones, P. P.; Majer, J. R. *Trans. Faraday Soc.* **1961**, *57*, 23.
- (26) Benson, S. W.; Cruickshank, F. R.; Golden, D. M.; Haugen, G. R.; O'Neal, H. E.; Rodgers, A. S.; Shaw, R.; Walsh, R. *Chem. Rev.* **1969**, *69*, 279.